symmetry

MDPI

Article

Thermally Controlled Synthesis of Octahedral Rhenium Clusters with 4,4′-Bipyridine and CN^- Apical Ligands

Anton A. Ulantikov [1], Taisiya S. Sukhikh [1], Evgeniy N. Gribov [2], Natalia V. Maltseva [2], Konstantin A. Brylev [1], Yuri V. Mironov [1,*] and Yakov M. Gayfulin [1,*]

[1] Nikolaev Institute of Inorganic Chemistry SB RAS, 3, Acad. Lavrentiev Ave., 630090 Novosibirsk, Russia; ulantikov@niic.nsc.ru (A.A.U.); sukhikh@niic.nsc.ru (T.S.S.); brylev@niic.nsc.ru (K.A.B.)

[2] Boreskov Institute of Catalysis SB RAS, 5, Acad. Lavrentiev Ave., 630090 Novosibirsk, Russia; gribov@catalysis.ru (E.N.G.); maltseva.n.v@catalysis.ru (N.V.M.)

* Correspondence: yuri@niic.nsc.ru (Y.V.M.); gayfulin@niic.nsc.ru (Y.M.G.)

Abstract: The selective preparation, structural and spectroscopic study of two new rhenium cluster complexes *trans*-$[Re_6S_8(bpy)_4(CN)_2]$ and *trans*-$[Re_6S_8(bpy)_2(CN)_4]^{2-}$ (bpy = 4,4′-bipyridine) obtained by reactions of corresponding hexarhenium cyanohalides with molten bpy are reported. The complexes were crystallized as solvates, displaying supramolecular structures based on cluster units linked by numerous weak interactions with bpy molecules. The molecular compound *trans*-$[Re_6S_8(bpy)_4(CN)_2]$ (**1**) is insoluble in water and common organic solvents, while the ionic compound *trans*-$Cs_{1.7}K_{0.3}[Re_6S_8(bpy)_2(CN)_4]$ (**2**) is somewhat soluble in DMSO, DMF and N-methylpyrrolidone. The presence of the redox-active ligand bpy leads to the occurrence of multi-electron reduction transitions in a solution of **2** at moderate potential values. The ambidentate CN^- ligand is the secondary functional group, which has potential for the synthesis of coordination polymers based on the new cluster complexes. In addition, both new compounds show a weak red luminescence, which is characteristic of complexes with a $\{Re_6S_8\}^{2+}$ cluster core.

Keywords: rhenium cluster; redox-active ligands; crystal structure; electronic structure

Citation: Ulantikov, A.A.; Sukhikh, T.S.; Gribov, E.N.; Maltseva, N.V.; Brylev, K.A.; Mironov, Y.V.; Gayfulin, Y.M. Thermally Controlled Synthesis of Octahedral Rhenium Clusters with 4,4′-Bipyridine and CN^- Apical Ligands. *Symmetry* **2021**, *13*, 2187. https://doi.org/10.3390/sym13112187

Academic Editor: Federico Palazzetti

Received: 19 October 2021
Accepted: 8 November 2021
Published: 16 November 2021

1. Introduction

The synthesis of molecular complexes of transition metals with redox-active ligands is one of the current major directions of inorganic chemistry. Due to the ability to accept electrons reversibly with changes in spectroscopic and magnetic properties, such compounds can be used in electrocatalysis [1,2] for the generation of free radicals and bistable systems [3] and as components of electrolytes [4]. Understanding the mutual influence of the transition metal cation and ligand composition on the electronic structure of the complex, the number and position of electrochemical transitions plays a crucial role in the study of the properties of redox-active complexes.

Over recent years, the physical and chemical properties of complexes based on octahedral cluster cores $\{Re_6Q_8\}^{2+}$ (Q = S or Se) have attracted a lot of attention [5]. These clusters are composed of an octahedral metallocluster $Re^{III}{}_6$ consisting of rhenium atoms linked by covalent bonds. Eight chalcogen atoms coordinate the faces of the Re_6 octahedron in the μ_3 mode. Each rhenium atom can be additionally coordinated by an apical ligand of an organic or inorganic nature. The cluster core is redox-active and capable of one-electron oxidation, with the formation of a 23-electron metal center $Re^{III}{}_5Re^{IV}$ [6–8]. The position of this transition is determined mainly by the type of chalcogenide ligands and weakly depends on the type of apical ligands. At the same time, variation of the apical ligands makes it possible to widely vary the solubility, reactivity, and spectroscopic properties of these complexes.

The $\{Re_6Q_8\}^{2+}$ cluster cores are Lewis acids and form complexes with N-donor organic ligands [9]. The study of the behavior of some redox-active N-donor ligands coordinated to

rhenium atoms has shown that they retain the ability to undergo reversible multielectron reduction. The potentials of the corresponding electrochemical transitions, as a rule, display a significant anodic shift [10]. This feature motivated us to study the mutual influence of the $\{Re_6Q_8\}^{2+}$ cluster core and coordinated redox-active ligands on the electrochemical properties of the resulting complexes. Earlier, several octahedral rhenium clusters containing the 4,4′-bipyridine (bpy) ligand as a model redox-active ligand were obtained in solution and studied in detail [11]. In our previous work, it was shown that the use of molten bpy makes it possible to obtain apically heteroleptic clusters containing four apical bpy ligands [12]. Here, we report the synthesis and investigation of these new apically heteroleptic hexarhenium cluster complexes simultaneously containing two functional ligands—namely, bpy and CN^-. An unusual finding in this work is the discovered ability of bpy molecules to replace the CN^- ligands of the precursor cluster $[Re_6S_8(CN)_4Cl_2]^{4-}$ during the melt synthesis, which is one of very few reports of the lability of CN^- ligands in the chemistry of octahedral rhenium clusters.

2. Experimental Section

Materials and methods. The cluster compound $Cs_{1.84}K_{1.16}(H)[Re_6S_8(CN)_4Cl_2]$ was synthesized following a previously reported procedure [13]. The DMSO (99.9%, Acros Organics) used for electrochemical investigations was stored over 3 Å molecular sieves in an Ar atmosphere. Other reagents and solvents were used as purchased.

Elemental analysis was made on a CHNS-O analyzer EuroEA3000 (EuroVector, Italy). IR spectra were recorded on a Bruker Scimitar FTS 2000 device (Bruker Corporation, Billerica, MA, USA) in KBr pellets over the range 4000–375 cm^{-1}. Energy dispersive spectroscopy (EDS) was performed using a Bruker Nano EDS analyzer paired with a Hitachi TM-3000 electron microscope (Hitachi, Ltd., Chiyoda City, Tokyo, Japan). UV-Vis spectra were recorded using an Agilent Cary 60 spectrophotometer (Agilent Technologies, Inc., USA) in DMSO solutions over the wavelength range 300–1000 nm. Luminescence spectra for the solid samples were recorded and the absolute emission quantum yields were estimated at ambient temperature using a Horiba Jobin Yvon Fluorolog 3 photoluminescence spectrometer (Horiba, Ltd., Kyoto, Japan), which includes an integration sphere, ozone-free Xe-lamp (450 W), cooled PC177CE-010 photon detection module with a PMT R2658 and double grating excitation and emission monochromators. Standard correction curves were used to correct excitation and emission spectra with respect to the source intensity (lamp and grating) and emission spectral response (detector and grating). Cyclic voltammetry was carried out on a Metrohm Autolab PGStat 302N (Netherlands) potentiostat-galvanostat with a built-in FRA analyzer (ECO Chemie, the Netherlands) voltammetry analyzer using a three-electrode scheme with carbon glass working, Pt auxiliary and Pt pseudoreference electrodes [14]. Investigations were carried out for $2 \cdot 10^{-4}$ M solutions of cluster salt **2** in 0.1 M Bu_4NPF_6 in DMSO under an Ar atmosphere. The registered value of $E_{1/2}$ for the Fc/Fc^+ couple was 0.130 V under these conditions.

*Preparation of trans-$[Re_6S_8(bpy)_4(CN)_2]$ (**1**):* $Cs_{1.84}K_{1.16}(H)[Re_6S_8(CN)_4Cl_2]$ (0.20 g, 0.1 mmol) and 4,4′-bipyridine (0.20 g, 1.0 mmol) were placed into a glass ampule. The sealed ampule was kept at 220 °C for 24 h and then cooled to room temperature. The reaction mixture contained orange crystals of *trans*-$[Re_6S_8(bpy)_4(CN)_2]\cdot 2bpy$ (**1·bpy**). Washing of the reaction mixture was carried out on a glass filter using boiling water (3 × 15 mL) and boiling EtOH (3 × 15 mL). The insoluble powder of compound **1** was dried in air. Yield (calculated on the precursor $Cs_{1.84}K_{1.16}(H)[Re_6S_8(CN)_4Cl_2]$): 0.21 g (95%). FT-IR (KBr, cm^{-1}): ν(CN) 2127.5; 4,4′-bipyridine: 1612.5, 1595.1, 1529.5, 1485.1, 1408.0, 1338.6, 1317.4, 1296.2, 1219.0, 1105.2, 1066.6, 1022.3, 999.1, 910.4, 854.5, 808.2, 729.1, 629.9, 570.9, 495.7; ν(ReS) 414.7. EDS (pellet): Re:S = 6.0:8.2. Elemental analysis calcd (%) for $C_{42}H_{32}N_{10}Re_6S_8$: C 24.6, H 1.6, N 6.8, S 12.5. Found: C 24.6, H 1.6, N 7.0, S 12.5%.

*Preparation of trans-$Cs_{1.7}K_{0.3}[Re_6S_8(bpy)_2(CN)_4]$ (**2**):* $Cs_{1.84}K_{1.16}(H)[Re_6S_8(CN)_4Cl_2]$ (0.20 g, 0.1 mmol) and 4,4′-bipyridine (0.20 g, 1.0 mmol) were placed into a glass ampule. The sealed ampule was kept at 130 °C for 48 h and then cooled to room temperature. The reaction mixture

contained orange crystals of *trans*-$Cs_{1.7}K_{0.3}[Re_6S_8(CN)_4(bpy)_2]\cdot 8bpy$ (**2·bpy**). Similarly with the purification of compound **1**, the reaction mixture was washed with boiling water and EtOH on a glass filter. After that, the residue was dissolved in 10 mL of DMSO to dissolve compound **2**. The solution was centrifuged to remove the insoluble black by-product, evaporated to 2 mL, and precipitated with ethanol to obtain the compound **2**. Yield (calculated on the precursor $Cs_{1.84}K_{1.16}(H)[Re_6S_8(CN)_4Cl_2]$): 0.14 g (65%). FT-IR (KBr, cm^{-1}): ν(CN) 2125.5; 4,4′-bipyridine: 1612.5, 1595.1, 1529.5, 1485.2, 1408.0, 1336.7, 1317.4, 1294.2, 1217.1, 1107.1, 1066.6, 1045.4, 1020.3, 950.9, 852.5, 808.2, 729.1, 626.9, 570.9, 497.6; ν(ReS) 414.7. EDS (pellet): Cs/K/Re/S = 1.9:0.5:6.0:8.3. Elemental analysis calcd (%) for $C_{24}H_{16}N_8Re_6S_8Cs_{1.7}K_{0.3}$: C 14.2, H 0.8, N 5.5, S 12.7. Found: C 14.5, H 0.8, N 5.6, S 12.7%.

Single-crystal diffraction studies. Single-crystal XRD data were collected at 150 K using a Bruker Apex DUO device (Bruker Corporation, USA) equipped with a 4 K CCD area detector. Graphite-monochromated MoKα radiation (λ = 0.71073 Å) was employed. The φ- and ω-scan techniques were used to measure intensities. Absorption corrections were applied by the SADABS program [15–17]. The crystal structures of **1·bpy** and **2·bpy** were solved using the SHELXT [18] and were refined using SHELXL [19] programs with OLEX2 GUI [20]. Atomic displacement parameters for non-hydrogen atoms were refined anisotropically excepti of those for cocrystal molecules. The structure of **1·bpy** revealed a 50/50% disorder of lattice bpy molecules. The AFIX command was applied to C_5N cycles of these bipyridine molecules. The crystallographic data and details of the structure refinements are summarized in Table 1. CCDC 2113087–2113088 contain the crystallographic data for compounds **1·bpy** and **2·bpy**, respectively. These data can be obtained free of charge from The Cambridge Crystallographic Data Centre via www.ccdc.cam.ac.uk/structures (accessed on 30 September 2021).

Table 1. Crystallographic data for the compounds **1·bpy** and **2·bpy**.

Compound	1·bpy	2·bpy
Empirical formula	$C_{62}H_{48}N_{14}Re_6S_8$	$C_{104}H_{80}N_{24}Re_6S_8Cs_{1.7}K_{0.3}$
Formula weight	2362.82	3273.52
Crystal system, space group	triclinic, *P*1	triclinic, *P*1
a/Å	10.2446 (3)	12.9047 (4)
b/Å	11.7046 (4)	14.3578 (5)
c/Å	14.4547 (4)	15.6379 (5)
α/°	74.479 (1)	64.637 (1)
β/°	80.385 (1)	82.959 (1)
γ/°	75.696 (1)	75.706 (1)
Volume/Å^3	1608.79 (9)	2536.64
Z	1	1
ρ_{calc}/g·cm^{-3}	2.439	2.143
μ/mm^{-1}	11.554	7.957
F (000)	1096	1548
Crystal size/mm^3	0.04 × 0.04 × 0.04	0.08 × 0.04 × 0.03
2Θ range for data collection/°	2.06 to 33.14	1.61 to 25.03
Index ranges	$-13 \leq h \leq 15$, $-17 \leq k \leq 18$, $-18 \leq l \leq 22$	$-15 \leq h \leq 15$, $-17 \leq k \leq 17$, $-18 \leq l \leq 18$
Reflections collected	37,931	26,949
Independent reflections	12,162 R_{int} = 0.0416 R_{sigma} = 0.0492	8954 R_{int} = 0.0409 R_{sigma} = 0.0442
Goodness-of-fit on F^2	1.025	1.044
Final *R* indexes [$I \geq 2\sigma$ (*I*)]	R_1 = 0.0322 wR_2 = 0.0547	R_1 = 0.0513 wR_2 = 0.1319
Final *R* indexes [all data]	R_1 = 0.0468 wR_2 = 0.0610	R_1 = 0.0729 wR_2 = 0.1537
Largest diff. peak/hole/e·Å^{-3}	1.58/−0.99	3.38/−1.28

Computational details. Density functional theory (DFT) calculations were carried out for *trans*-$[Re_6S_8(bpy)_2(CN)_4]^{2-}$ and *trans*-$[Re_6S_8(bpy)_4(CN)_2]$ clusters in a solvent (acetonitrile) environment in the ADF2017 program package [21,22]. Geometric parameters for the clusters were optimized with a VWN+S12g dispersion-corrected density functional [23–25] and all-electron TZP basis set [26] in C_1 symmetry. No imaginary frequencies were found in the calculated vibrational spectra. Single point calculations of bonding energies and molecular orbitals were made with a dispersion-corrected hybrid density functional S12h and all-electron TZP basis set [25,26] with geometries from the VWN+S12g/TZP level of theory. The solvent environment (acetonitrile) was simulated by the COSMO method [27]. Zero order regular approximation (ZORA) was used to take the scalar relativistic effects into account [28].

3. Results and Discussion

3.1. Synthesis

The substitution of terminal halide ligands in $[Re_6Q_8X_6]^{4-/3-}$ clusters, where X are Cl^-, Br^- or I^-, by organic ligands is a convenient method for modifying the properties of these complexes. It has been found that the use of molten organic compounds as a reaction media leads to different products from these reactions depending on type of the compound used. As a rule, aprotic compounds lead to the formation of electrically neutral molecular clusters $[Re_6Q_8X_2L_4]$ [12,29,30]. At the same time, melts of protonic proligands often give completely substituted homoleptic products $[Re_6Q_8L_6]^n$ [31–33].

In this work, an apically heteroleptic cluster *trans*-$[Re_6S_8(CN)_4Cl_2]^{4-}$ was used as a starting material. A feature of this cluster is the simultaneous presence of relatively labile chloride ligands in the *trans*-positions, while the equatorial positions are occupied by strongly coordinating cyanide ligands. Thus, it may be possible to selectively substitute two chloride anions to 4,4′-bipyridine (bpy). We showed recently that the reaction of $[Re_6Q_8X_6]^{4-}$ (X = Cl or Br) clusters with bpy requires quite high temperatures of 220 °C for the quantitative formation of final four-substituted neutral complexes with the general formula *trans*-$[Re_6Q_8(bpy)_4X_2]$ [12]; therefore, we carried out the reaction between $Cs_{1.8}K_{1.2}(H)[Re_6S_8(CN)_4Cl_2]$ and bpy at 220 °C. As a result, a crystalline product, **1·bpy,** was formed, which contained the neutral cluster fragment *trans*-$[Re_6S_8(bpy)_4(CN)_2]$ in its structure. Thorough purification of this compound led to the obtaining of insoluble compound **1**. Elemental analysis confirmed that formation of the tetrasubstituted product occurred in nearly quantitative yields. Therefore, bpy molecules substituted two chloride and two cyanide ligands in the $[Re_6S_8(CN)_4Cl_2]^{4-}$ precursor. We supposed that a decrease in the reaction temperature could lead to selective substitution of only two relatively labile halide ligands. Indeed, having carried out the synthesis at 130 °C, we obtained the crystalline product *trans*-$Cs_{1.7}K_{0.3}[Re_6S_8(bpy)_2(CN)_4]\cdot 3.5$ bpy (**2 bpy**). Dissolution of **2 bpy** in DMSO, followed by precipitation with EtOH, led to the formation of the pure compound **2**, which was obtained with a decent yield.

To the best of our knowledge, the synthesis of compound **1** is the first evidence of a substitution of apical cyanide anions in octahedral clusters of rhenium, and along with compound **2,** is the first example of a thermally controlled selective substitution of two or four apical ligands. Earlier, a similar substitution was shown to be possible in the case of heterometallic rhenium-molybdenum octahedral clusters [34]. There are also examples of crystalline compounds *trans*-$[Re_6S_8(CN)_2L_4]$ (L = pyridine, 4-methylpyridine) obtained by the reaction of polymeric complex $[Re_6S_8(CN)_4S_{2/2}]^n$ with a corresponding organic compound [35]. However, these compounds were obtained as several crystals of the by-product, while the main reaction products were identified as disubstituted clusters of *trans*-$[Re_6S_8(CN)_4L_2]$.

3.2. Luminescence

Compounds **1** and **2** exhibit very weak luminescence in the red region at excitation wavelengths of 355 nm. The emission peak values are roughly 690 and 700 nm for

compounds **1** and **2**, respectively, which is typical for octahedral rhenium chalcogenide clusters [4]. The negligible intensity of the photoluminescence did not allow us to determine the emission lifetimes and quantum yields.

3.3. Crystal Structures

Compound **1·bpy** crystallizes in a triclinic system, space group *P*1. The asymmetric fragment contains half of the cluster—three rhenium atoms, four sulfur atoms, two coordinated bpy molecules, and one CN^- group. The asymmetric fragment also contains one solvate bpy molecule, which is disordered over two positions. All atoms of the asymmetric fragment lie in general positions. Four bpy molecules are coordinated to the metal atoms of the cluster core in the equatorial plane, forming Re–N bonds with typical lengths of 2.18–2.19 Å. One of the coordinated bpy molecules is disordered due to a rotation of the outer ring (Figure 1). Two cyanide groups are coordinated in a *trans* position, with a Re–C bond length of 2.13 Å.

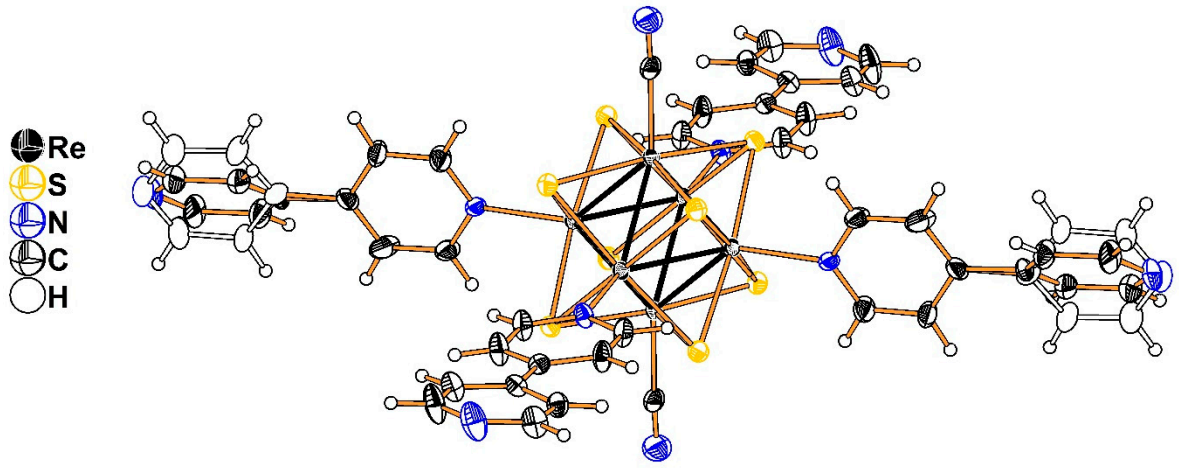

Figure 1. ORTEP structure of the cluster complex *trans*-$[Re_6S_8(bpy)_4(CN)_2]$ in **1·bpy**. Alternative position of disordered pyridine rings depicted as contours. Atomic displacement ellipsoids of 50% probability are shown.

The packing of **1·bpy** is formed by CH...π interactions between perpendicularly oriented bpy ligands of neighboring cluster anions (Figure 2a) and by π-stacking between parallel oriented ligands (Figure 2b). The CH ... π interactions are characterized by a distance of 3.88 Å between a corresponding ring centroid and the nearest carbon atom of its neighboring molecule. Distances between centroids of parallel rings are 3.33–3.67 Å. Cyanide groups form weak CH ... N hydrogen bonds of a length of 3.21 Å with bpy ligands of neighboring cluster fragments. The solvate bpy molecules occupy voids in the structure and form π-stacking contacts with coordinated bpy molecules.

Compound **2·bpy** crystallizes in a triclinic crystal system, space group $P\,\bar{1}$. The asymmetric fragment contains half of cluster fragment—three rhenium atoms, four sulfur atoms, one coordinated bpy molecule and two CN^- groups. In addition, the asymmetric fragment includes eight solvate bpy molecules and one alkali metal cation position, which is occupied by K and Cs atoms at a ratio of 0.17/0.83. Two bpy ligands are coordinated in a *trans*-position with a Re–N bond length of 2.21 Å. The torsion angle between bpy rings is 144.0°. Four cyanide groups are coordinated in the equatorial plane and form Re–C bonds with lengths of 2.13–2.15 Å (Figure 3).

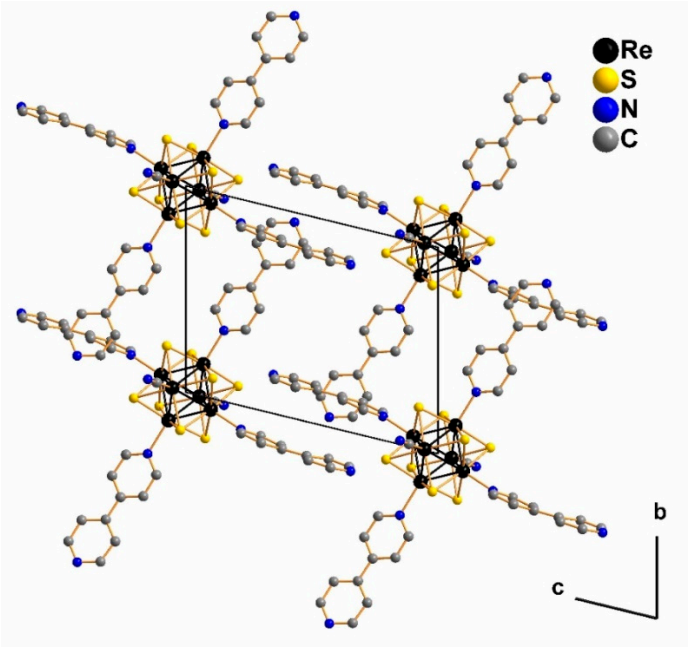

(**a**)

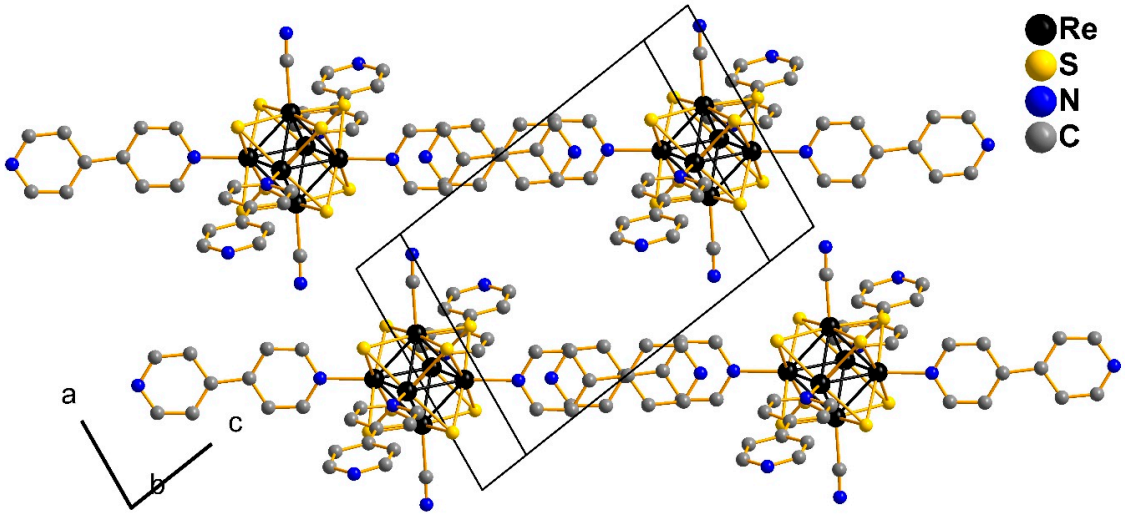

(**b**)

Figure 2. Packing of cluster fragments in the structure of compound **1·bpy** in bc plane (**a**) and in direction perpendicular to bpy ligands connected by π-stacking (**b**). Solvate bpy molecules, hydrogen atoms and disordered pyridine rings are not shown for clarity.

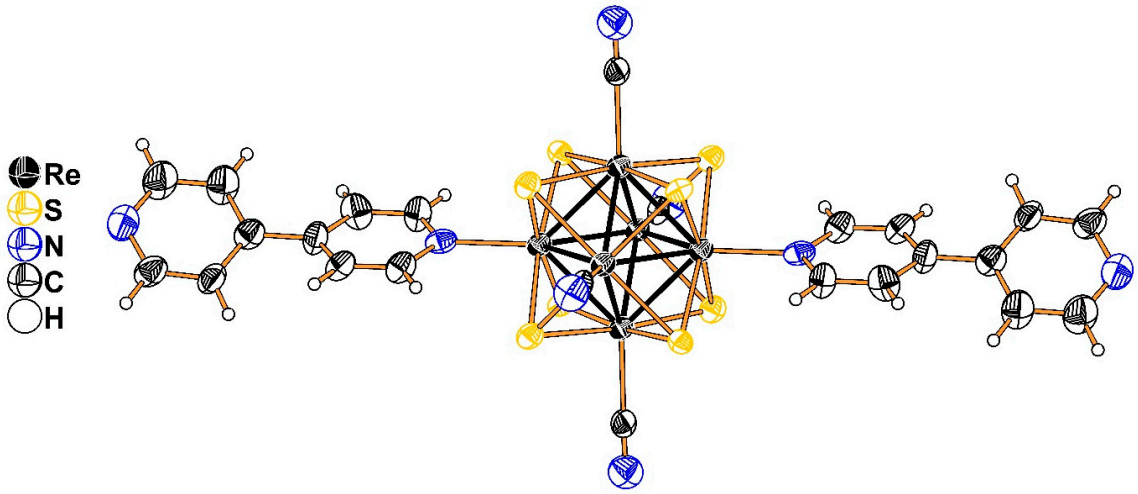

Figure 3. ORTEP structure of the cluster complex *trans*-$[Re_6S_8(bpy)_2(CN)_4]^{2-}$ in **2·bpy**. Thermal ellipsoids of 50% probability are shown.

Compound **2·bpy** represents a rare example of a Cs cation surrounded in crystal by N-donor ligands only [36–39], and is the first example of the bridging mode of a 4,4′-bypiridine molecule between two alkaline metal sites. The coordination environment of each Cs/K position consists of two N atoms of CN^- ligands, one N atom of an apical bpy ligand and four N atoms of solvate bpy molecules, forming a monocapped trigonal prism. The corresponding Cs/K . . . N distances are 3.23, 3.40 and 3.22–3.24 Å, respectively. The nitrogen atoms of two solvate bpy molecules and two CN^- ligands are in bridging coordination between two Cs/K ions related by the inversion center (0, 0, $\frac{1}{2}$). Crystal packing of this compound is formed by the Cs/K···N interactions, π stacking between coordinated and solvate bpy molecules, and hydrogen bonds between N atoms of CN^- ligands and H atoms of aromatic rings (Figure 4). The corresponding π stacking distances between ring centroids lie in the range of 3.66–3.71 Å, while C–H . . . N distances between C and N atoms are 3.50–3.57 Å. It is interesting to note that there is no π stacking between the bpy ligands of neighboring cluster fragments.

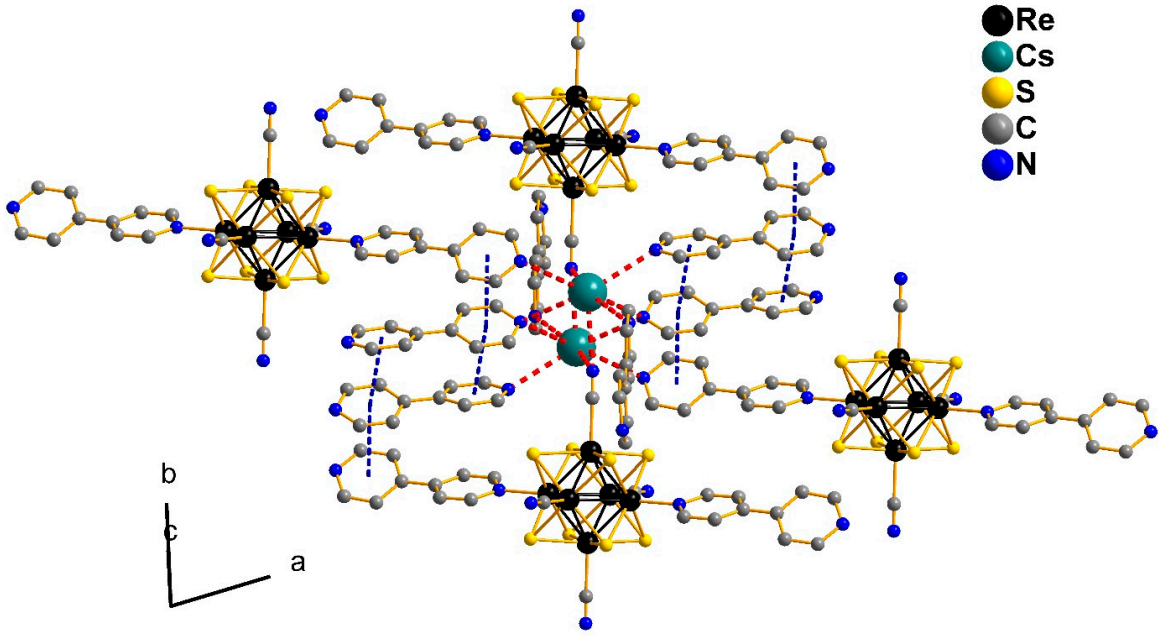

Figure 4. Visualization of weak interactions in the structure of compound **2·bpy**. Red: Cs/K . . . N contacts, blue: contacts between pyridine rings. Hydrogen atoms are not shown.

3.4. Electronic Structure

Electronic structures of *trans*-$[Re_6S_8(bpy)_2(CN)_4]^{2-}$ and *trans*-$[Re_6S_8(bpy)_4(CN)_2]$ clusters in the near frontier region are characterized by the presence of the $\{Re_6S_8\}$-centered, almost degenerated HOMO and HOMO–1, lying at notable distances (close to 0.7 eV) from the underlying orbitals (Figure 5a). Two (for *trans*-$[Re_6S_8(bpy)_2(CN)_4]^{2-}$) or four (for *trans*-$[Re_6S_8(bpy)_4(CN)_2]$) of the lowest unoccupied orbitals are localized mainly on the pairs of bpy ligands in the *trans*-positions (Figure 5b,c). HOMO–LUMO gaps (3.47 and 3.59 eV for $[Re_6S_8(bpy)_2(CN)_4]^{2-}$ and $[Re_6S_8(bpy)_4(CN)_2]$, respectively) are comparable with those for $\{Re_6Q_8\}^{2+}$-based clusters, with an inorganic apical ligand environment [40], and are much larger than those for $[Re_6Q_8bpy_4X_2]$ (Q = S or Se; X = Cl or Br) clusters [12]. It is interesting to note that LUMOs for both new clusters show a significant contribution of Re *d*-orbitals (~15%) and have bonding characteristics in the Re–N direction. This fact contrasts with the electronic structures of $[Re_6Q_8bpy_4X_2]$ clusters, which also contain LUMO–LUMO+3, localized mainly on the pairs of bpy ligands in the *trans*-positions, but with a negligible contribution of Re and Q atomic orbitals. Another interesting feature of the new cluster in comparison with $[Re_6Q_8bpy_4X_2]$ molecules is the absence of a pronounced gap between the bpy-centered unoccupied orbitals and overlying orbitals. Potentially, this could cause the metal-to-ligand charge transfer (MLCT) weak-type emission of the new clusters in a similar way to that reported for *cis*- and *trans*-$[Re_6S_8Cl_4(bpy)_2]$ anions [41].

3.5. Redox Behavior of $[Re_6S_8(bpy)_2(CN)_4]^{2-}$ Cluster Anions

It was found that compound **1** is insoluble in polar and non-polar organic solvents, probably due to a number of weak interactions between neutrally charged cluster fragments. Compound **2** was found to be slightly soluble in DMSO, DMF and N-methylpyrrolidone. Free 4,4′-bipyridine in DMSO solution shows successive one-electron reduction processes at $E_{1/2} = -2.29$ and -2.74 V vs. the Fc/Fc^+ couple, corresponding to the formation of $bpy^{\bullet-}$ and bpy^{2-} anions, respectively [42]. The cyclic voltammogram of compound **2** in DMSO (Figure 6) revealed a complicated set of reversible and quasi-reversible redox transitions at potentials from -1.2 to -2.3 V. The peak current potential of the first transition is shifted by almost +0.9 V from the corresponding transition of free bpy. This shift is close to ones previously reported for Re_6 clusters with bpy ligands [11,12] and is caused by the strong Lewis acidity of the $\{Re_6S_8\}^{2+}$ cluster core. Noteworthily, we did not observe any transitions in the positive region; this means that the reversible oxidation of the $\{Re^{III}{}_6\}/\{Re^{III}{}_5Re^{IV}\}$ cluster core, which is common for octahedral rhenium clusters [43], is either blocked or is outside the available potential window.

Due to the low solubility of compound **2** and the relatively large background current, direct measurement of the electron count transferred in the redox transitions by coulometry was inapplicable. The total number of electrons n for these reduction processes has been estimated using the formula $i_p = 2.69 \cdot 10^5 n^{3/2} A D_0{}^{1/2} C_0{}^* \nu^{1/2}$, where A is the working electrode surface area (0.0314 cm^2), D_0 is the diffusion coeffiient of the cluster anion, and C_0 is the cluster anion concentration ($2 \cdot 10^{-7}$ $mol \cdot cm^{-1}$) [44]. The peak current values i_p of the two most intense reduction transitions at -2.35 and -3.40 V vs. Fc/Fc^+ (Figure 6) have been corrected for capacitive charging of the electrode surface in a blank electrolyte solution at -1.0 V, using the formula $\Delta i_p = (i_a - i_c)/2$. The diffusion coefficient D_0 for $[Re_6S_8(bpy)_2(CN)_4]^{2-}$ cluster was estimated using the Stokes–Einstein formula $D_0/D_{Fc} = r_{Fc}/r_0$, where $D_{Fc} = 6{,}7 \cdot 10^{-6}$ $cm \cdot s^{-1}$ [45,46], and $r_{Fc} = 2.25$ Å, $r_0 = 11.35$ Å (taking into account Van der Waals radii). The resulting number of electrons n calculated in this way is 1.4 and 1.9 for transitions at -2.35 and -3.40 V, respectively, yielding a total number of 3.3 e per cluster unit. Considering the presence of less intense transitions, this result is in good agreement with the expected number of four electrons per cluster unit. At the same time, estimation of the total number of electrons using the approximation of i_p as $i_p = i_{ch} * \nu + i_F * \nu^{1/2}$, where i_p is the peak current, i_{ch} is the current of double layer charging, and i_F is the current of the Faraday process [47], yielded 2.0 e and 2.6 e for transitions at -2.35 and -3.40 V, respectively, yielding a total number of 4.6 e per cluster unit.

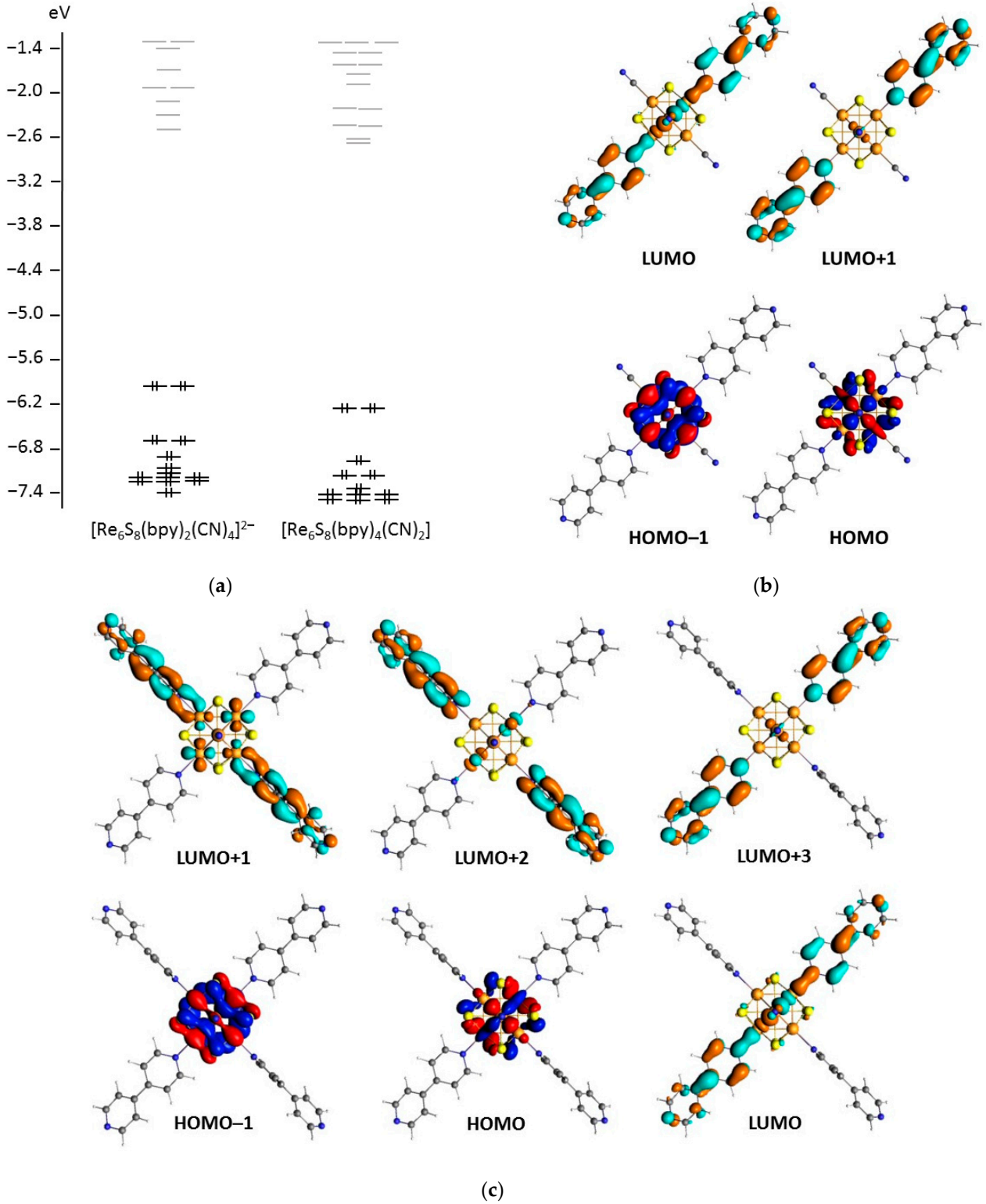

Figure 5. Energy levels diagram for *trans*-$[Re_6S_8(bpy)_2(CN)_4]^{2-}$ and *trans*-$[Re_6S_8(bpy)_4(CN)_2]$ clusters (**a**); molecular orbitals of *trans*-$[Re_6S_8(bpy)_2(CN)_4]^{2-}$ (**b**) and *trans*-$[Re_6S_8(bpy)_4(CN)_2]$ (**c**) clusters in near frontier region.

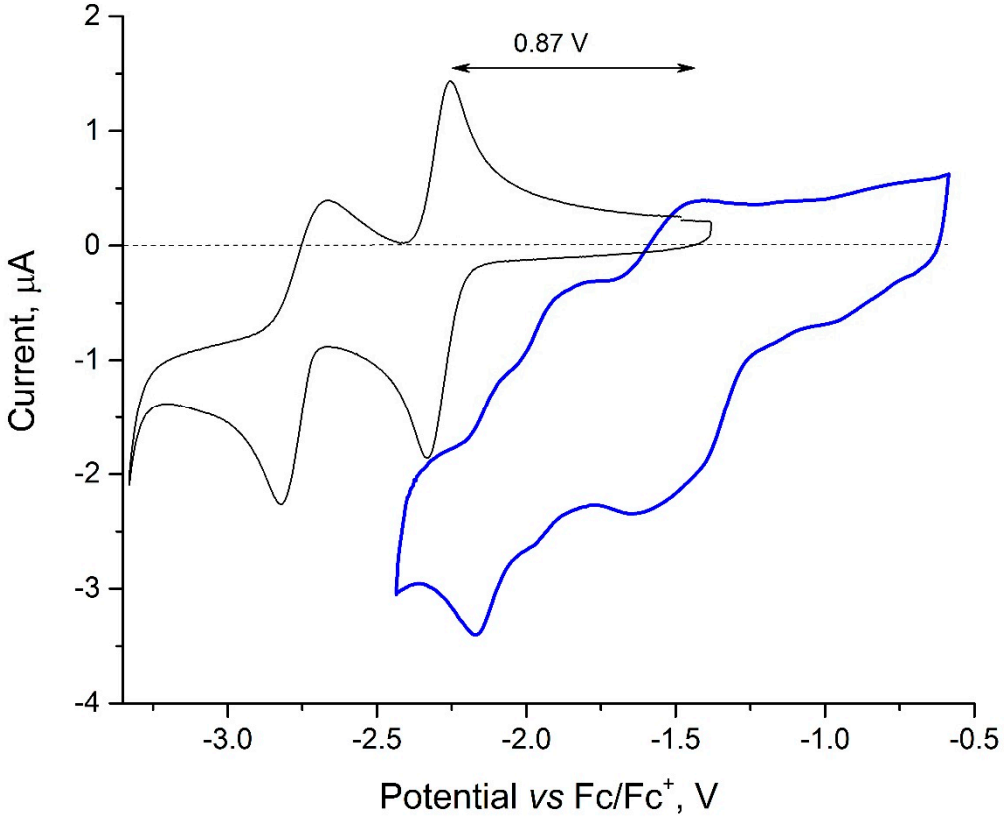

Figure 6. Cyclic voltammogram of compound **2** (blue) and free 4,4′-bipyridine (black) in DMSO solution. Scan rate was 0.1 V·s^{-1}; dashed line marks zero current level. Series of low-intensity reduction transitions from −0.5 to −1.2 V is caused by traces of molecular oxygen in Ar gas.

4. Conclusions

The reaction of the heteroligand chalcogenide octahedral rhenium cluster $[Re_6S_8(CN)_4Cl_2]^{4-}$ with the 4,4′-bipyridine melt reveals the possibility of replacing inert cyanide anions as well as relatively labile halide ligands by bpy molecules. It was found that the number of substituted ligands depends on the reaction temperature. At a relatively low temperature, only halide ligands are replaced with the formation of anionic cluster *trans*-$[Re_6S_8(bpy)_2(CN)_4]^{2-}$, while at a higher temperature, a molecular cluster *trans*-$[Re_6S_8(bpy)_4(CN)_2]$ forms. This reaction is the first example of the substitution of cyanide anions coordinated to the octahedral rhenium cluster.

The $Cs_{1.7}K_{0.3}[Re_6S_8(CN)_4(bpy)_2]\cdot 3.5bpy$ (**2·bpy**) compound demonstrates a rare example of a compound containing a Cs^+ cation surrounded by only N-donor ligands in the crystal structure. Moreover, the packing of this compound contains dimeric fragments in which the Cs^+/K^+ cations are connected by bridging bpy molecules. The electronic structures of these new compounds are characterized by the presence of unoccupied orbitals localized mainly on the bpy ligands. However, in contrast to the previously known rhenium clusters of this ligand, the structure of LUMO and LUMO+1 contains a significant contribution of rhenium *d*-orbitals. An electrochemical study of the *trans*-$[Re_6S_8(bpy)_2(CN)_4]^{2-}$ anion in DMSO solution showed that the reduction potential of bpy ligands undergoes a strong shift toward the anodic region as compared to molecular bpy in solution.

Author Contributions: Realization of the experiments and analysis of the experimental data, A.A.U., N.V.M. and E.N.G.; calculation of the electronic structures, Y.M.G.; investigation of luminescence properties K.A.B.; investigation of crystal structures, T.S.S.; draft preparation, A.A.U. and Y.M.G.; manuscript editing, Y.M.G. and K.A.B.; conceptualization and supervision, Y.V.M. All authors have read and agreed to the published version of the manuscript.

Funding: This work was financially supported by the Russian Foundation for Basic Research (project 20-33-70112). Luminescence measurements were supported by a grant from the Russian Science Foundation (project 19-73-20196). Measurements were performed in the "Center for Optical and Laser materials research" (St. Petersburg State University, St. Petersburg, Russian Federation). The research (Nikolaev Institute of Inorganic Chemistry SB RAS) was supported by the Ministry of Science and Higher Education of the Russian Federation, N. 121031700321-3 and 121031700313-8.

Data Availability Statement: The crystallographic data and details of the structure refinements are summarized in Table 1. CCDC 2113087–2113088 contain the crystallographic data for compounds **1·bpy** and **2·bpy**, respectively. These data can be obtained free of charge from The Cambridge Crystallographic Data Centre via www.ccdc.cam.ac.uk/structures.

Conflicts of Interest: The authors declare no conflict of interest.

References

1. Costentin, C.; Robert, M.; Savéant, J.-M. Molecular catalysis of electrochemical reactions. *Curr. Opin. Electrochem.* **2017**, *2*, 26–31. [CrossRef]
2. Dalle, K.E.; Warnan, J.; Leung, J.J.; Reuillard, B.; Karmel, I.S.; Reisner, E. Electro- and Solar-Drien Fuel Synthesis with First Row Transition Metal Complexes. *Chem. Rev.* **2019**, *119*, 2752–2875. [CrossRef] [PubMed]
3. Starikova, A.A.; Minkin, V.I. Adducts of transition metal complexes with redox-active ligands: The structure and spin-state-switching rearrangements. *Russ. Chem. Rev.* **2018**, *87*, 1049–1079. [CrossRef]
4. Cameron, J.M.; Holc, C.; Kibler, A.J.; Peake, C.L.; Walsh, D.A.; Newton, G.N.; Johnson, L.R. Molecular redox species for next-generation batteries. *Chem. Soc. Rev.* **2021**, *50*, 5863–5883. [CrossRef]
5. Cordier, S.; Molard, Y.; Brylev, K.A.; Mironov, Y.V.; Grasset, F.; Fabre, B.; Naumov, N.G. Advances in the Engineering of Near Infrared Emitting Liquid Crystals and Copolymers, Extended Porous Frameworks, Theranostic Tools and Molecular Junctions Using Tailored Re6 Cluster Building Blocks. *J. Clust. Sci.* **2015**, *26*, 53–81. [CrossRef]
6. Long, J.R.; McCarty, L.S.; Holm, R.H. A Solid-State Route to Molecular Clusters: Access to the Solution Chemistry of $[Re_6Q_8]^{2+}$ (Q = S, Se) Core-Containing Clusters via Dimensional Reduction. *J. Am. Chem. Soc.* **1996**, *118*, 4603–4616. [CrossRef]
7. Naumov, N.G.; Ostanina, E.V.; Virovets, A.V.; Schmidtman, M.; Müller, A.; Fedorov, V.E. 23-Electron Re_6 metal clusters: Syntheses and crystal structures of $(Ph_4P)_3[Re_6S_8(CN)_6]$, $(Ph_4P)_2(H)[Re_6Se_8(CN)_6]\cdot 8H_2O$, and $(Et_4N)_2(H)[Re_6Te_8(CN)_6]\cdot 2H_2O$. *Russ. Chem. Bull.* **2002**, *51*, 866–871. [CrossRef]
8. Amela-Cortes, M.; Cordier, S.; Naumov, N.G.; Mériadec, C.; Artzner, F.; Molard, Y. Hexacyano octahedral metallic clusters as versatile building blocks in the design of extended polymeric framework and clustomesogens. *J. Mater. Chem. C* **2014**, *2*, 9813–9823. [CrossRef]
9. Szczepura, L.F.; Soto, E. *Ligated Transition Metal Clusters in Solid-State Chemistry: The Legacy of Marcel Sergent*; Halet, J.-F., Ed.; Springer International Publishing: Cham, Switzerland, 2019; pp. 75–108.
10. Yoshimura, T.; Umakoshi, K.; Sasaki, Y.; Sykes, A.G. Synthesis, Structures, and Redox Properties of Octa(μ_3-sulfido)hexarhenium(III) Complexes Having Terminal Pyridine Ligands. *Inorg. Chem.* **1999**, *38*, 5557–5564. [CrossRef] [PubMed]
11. Yoshimura, T.; Umakoshi, K.; Sasaki, Y.; Ishizaka, S.; Kim, H.-B.; Kitamura, N. Emission and Metal- and Ligand-Centered-Redox Characteristics of the Hexarhenium(III) Clusters trans- and *cis*-$[Re_6(\mu_3\text{-}S)_8Cl_4(L)_2]^{2-}$, Where L Is a Pyridine Derivative or Pyrazine. *Inorg. Chem.* **2000**, *39*, 1765–1772. [CrossRef]
12. Ulantikov, A.A.; Gayfulin, Y.M.; Ivanov, A.A.; Sukhikh, T.S.; Ryzhikov, M.R.; Brylev, K.A.; Smolentsev, A.I.; Shestopalov, M.A.; Mironov, Y.V. Soluble Molecular Rhenium Cluster Complexes Exhibiting Multistage Terminal Ligands Reduction. *Inorg. Chem.* **2020**, *59*, 6460–6470. [CrossRef]
13. Naumov, N.G.; Ledneva, A.Y.; Kim, S.-J.; Fedorov, V.E. New *trans*-$[Re_6S_8(CN)_4L_2]^{n-}$ Rhenium Cluster Complexes: Syntheses, Crystal Structures and Properties. *J. Clust. Sci.* **2009**, *20*, 225–239. [CrossRef]
14. Kasem, B.K.K.; Jones, S. Platinum as a Reference Electrode in Electrochemical Measurements. *Platin. Met. Rev.* **2008**, *52*, 100–106. [CrossRef]
15. *APEX2. Version 2.0*; Bruker Advanced X-ray Solutions: Madison, WI, USA, 2000.
16. *SAINT. Version 8.18c*; Bruker Advanced X-ray Solutions: Madison, WI, USA, 2012.
17. *SADABS. Version 2.11*; Bruker Advanced X-ray Solutions: Madison, WI, USA, 2000.
18. Sheldrick, G. SHELXT—Integrated space-group and crystal-structure determination. *Acta Cryst. A* **2015**, *71*, 3–8. [CrossRef]
19. Sheldrick, G. Crystal structure refinement with SHELXL. *Acta Cryst. C* **2015**, *71*, 3–8. [CrossRef] [PubMed]
20. Dolomanov, O.V.; Bourhis, L.J.; Gildea, R.J.; Howard, J.A.K.; Puschmann, H. OLEX2: A complete structure solution, refinement and analysis program. *J. Appl. Cryst.* **2009**, *42*, 339–341. [CrossRef]
21. Fonseca Guerra, C.; Snijders, J.G.; te Velde, G.; Baerends, E.J. Towards an order-N DFT method. *Theor. Chem. Acc.* **1998**, *99*, 391–403. [CrossRef]
22. Te Velde, G.; Bickelhaupt, F.M.; Baerends, E.J.; Fonseca Guerra, C.; van Gisbergen, S.J.A.; Snijders, J.G.; Ziegler, T. Chemistry with ADF. *J. Comput. Chem.* **2001**, *22*, 931–967. [CrossRef]

23. Vosko, S.H.; Wilk, L.; Nusair, M. Accurate spin-dependent electron liquid correlation energies for local spin density calculations: A critical analysis. *Can. J. Phys.* **1980**, *58*, 1200–1211. [CrossRef]
24. Perdew, J.P.; Wang, Y. Accurate and simple analytic representation of the electron-gas correlation energy. *Phys. Rev. B* **1992**, *45*, 13244–13249. [CrossRef]
25. Swart, M. A new family of hybrid density functionals. *Chem. Phys. Lett.* **2013**, *580*, 166–171. [CrossRef]
26. Van Lenthe, E.; Baerends, E.J. Optimized Slater-type basis sets for the elements 1–118. *J. Comput. Chem.* **2003**, *24*, 1142–1156. [CrossRef] [PubMed]
27. Pye, C.C.; Ziegler, T. An implementation of the conductor-like screening model of solvation within the Amsterdam density functional package. *Theor. Chem. Acc.* **1999**, *101*, 396–408. [CrossRef]
28. Lenthe, E.; Ehlers, A.; Baerends, E.-J. Geometry optimizations in the zero order regular approximation for relativistic effects. *J. Chem. Phys.* **1999**, *110*, 8943–8953. [CrossRef]
29. Ivanov, A.A.; Shestopalov, M.A.; Brylev, K.A.; Khlestkin, V.K.; Mironov, Y.V. A family of octahedral rhenium cluster complexes *trans*-[{Re_6Q_8}$(PPh_3)_4X_2$] (Q = S or Se, X = Cl, Br or I): Preparation and halide-dependent luminescence properties. *Polyhedron* **2014**, *81*, 634–638. [CrossRef]
30. Ulantikov, A.A.; Gayfulin, Y.M.; Sukhikh, T.S.; Ryadun, A.A.; Ryzhikov, M.R.; Mironov, Y.V. Synthesis, structure and physico-chemical properties of molecular rhenium cluster complexes with 4-phenylpyridine molecules as terminal ligands. *J. Struct. Chem.* **2021**, *62*, 1009–1019. [CrossRef]
31. Bardin, V.A.; Ivanov, A.A.; Konovalov, D.I.; Smolentsev, A.I.; Shestopalov, M.A. Crystal structure and luminescent properties of rhenium clusters [{$Re_6(\mu_3\text{-}Q)_8$}(imz-[1,2-a]py)$_6$]Br_2. *J. Struct. Chem.* **2020**, *61*, 1624–1629. [CrossRef]
32. Konovalov, D.I.; Ivanov, A.A.; Vorotnikov, Y.A.; Brylev, K.A.; Eltsov, I.V.; Kuratieva, N.V.; Kitamura, N.; Mironov, Y.V.; Shestopalov, M.A. Synthesis and luminescence properties of apically homoleptic octahedral rhenium clusters with pyrazole and 3,5-dimethylpyrazole. *Inorg. Chim. Acta* **2019**, *498*, 119128. [CrossRef]
33. Shestopalov, M.A.; Zubareva, K.E.; Khripko, O.P.; Khripko, Y.I.; Solovieva, A.O.; Kuratieva, N.V.; Mironov, Y.V.; Kitamura, N.; Fedorov, V.E.; Brylev, K.A. The First Water-Soluble Hexarhenium Cluster Complexes with a Heterocyclic Ligand Environment: Synthesis, Luminescence, and Biological Properties. *Inorg. Chem.* **2014**, *53*, 9006–9013. [CrossRef] [PubMed]
34. Muravieva, V.K.; Gayfulin, Y.M.; Lappi, T.I.; Dorcet, V.; Sukhikh, T.S.; Lemoine, P.; Ryzhikov, M.R.; Mironov, Y.V.; Cordier, S.; Naumov, N.G. Apical Cyanide Ligand Substitution in Heterometallic Clusters $[Re_3Mo_3Q_8(CN)_6]^{n-}$ (Q = S, Se). *Eur. J. Inorg. Chem.* **2019**, *2019*, 2685–2690. [CrossRef]
35. Ledneva, A.Y.; Naumov, N.G.; Virovets, A.V.; Cordier, S.; Molard, Y. Crystal structures of *trans*-$[Re_6S_8(CN)_2L_4]$ complexes, L = pyridine or 4-methylpyridine. *J. Struct. Chem.* **2012**, *53*, 132–137. [CrossRef]
36. Tadokoro, M.; Shiomi, T.; Isobe, K.; Nakasuji, K. Cesium(I)-Mediated 3-D Superstructures by One-Pot Self-Organization of Hydrogen-Bonded Nickel Complexes. *Inorg. Chem.* **2001**, *40*, 5476–5478. [CrossRef]
37. Poturovic, S.; Lu, D.; Heeg, M.J.; Winter, C.H. Synthesis and structural characterization of heavier group 1 methyl tetrazolate complexes: New bridging coordination modes of the tetrazolate ligand. *Polyhedron* **2008**, *27*, 3280–3286. [CrossRef]
38. Dechambenoit, P.; Ferlay, S.; Kyritsakas, N.; Hosseini, M.W. Molecular tectonics: Crystal engineering of mixed valence Fe(II)/Fe(III) solid solutions. *Chem. Commun.* **2010**, *46*, 868–870. [CrossRef] [PubMed]
39. Klapötke, T.M.; Stein, M.; Stierstorfer, J. Salts of 1H-Tetrazole—Synthesis, Characterization and Properties. *Z. Anorg. Allgem. Chem.* **2008**, *634*, 1711–1723. [CrossRef]
40. Rabanal-León, W.A.; Murillo-López, J.A.; Páez-Hernández, D.; Arratia-Pérez, R. Understanding the Influence of Terminal Ligands on the Electronic Structure and Bonding Nature in $[Re_6(\mu_3\text{-}Q_8)]^{2+}$ Clusters. *J. Phys. Chem. A* **2014**, *118*, 11083–11089. [CrossRef]
41. Yoshimura, T.; Suo, C.; Tsuge, K.; Ishizaka, S.; Nozaki, K.; Sasaki, Y.; Kitamura, N.; Shinohara, A. Excited-State Properties of Octahedral Hexarhenium(III) Complexes with Redox-active N-heteroaromatic Ligands. *Inorg. Chem.* **2010**, *49*, 531–540. [CrossRef]
42. Tabner, B.J.; Yandle, J.R. A correlation of half-wave reduction potentials with theoretical calculations for some nitrogen-containing heteromolecules in dimethylformamide. *J. Chem. Soc. A* **1968**, 381–388. [CrossRef]
43. Gabriel, J.-C.P.; Boubekeur, K.; Uriel, S.; Batail, P. Chemistry of Hexanuclear Rhenium Chalcohalide Clusters. *Chem. Rev.* **2001**, *101*, 2037–2066. [CrossRef]
44. Bard, A.J.; Faulkner, L.R. (Eds.) *Electrochemical Methods: Fundamentals and Applications, 2 ed.*; John Wiley & Sons, Inc.: Hoboken, NJ, USA, 2001.
45. Janisch, J.; Ruff, A.; Speiser, B.; Wolff, C.; Zigelli, J.; Benthin, S.; Feldmann, V.; Mayer, H.A. Consistent diffusion coefficients of ferrocene in some non-aqueous solvents: Electrochemical simultaneous determination together with electrode sizes and comparison to pulse-gradient spin-echo NMR results. *J. Solid State Electrochem.* **2011**, *15*, 2083. [CrossRef]
46. Tsierkezos, N.G. Cyclic Voltammetric Studies of Ferrocene in Nonaqueous Solvents in the Temperature Range from 248.15 to 298.15 K. *J. Solut. Chem.* **2007**, *36*, 289–302. [CrossRef]
47. Forghani, M.; Donne, S.W. Complications When Differentiating Charge Transfer Processes in Electrochemical Capacitor Materials: Assessment of Cyclic Voltammetry Data. *J. Electrochem. Soc.* **2019**, *166*, A1370–A1379. [CrossRef]